Proceedings of ERAD 2006

# Engineering description of a scanning, L-band, pulse-compression radar for clear-air atmospheric research

**J. D. Eastment[1], O. T. Davies[2], J. C. Nicol[3] and E. G. Pavelin[4]**

[1] Radio Communications Research Unit, CCLRC Rutherford Appleton Laboratory, Chilton, Didcot, Oxfordshire, OX11 0QX. (United Kingdom)

[2] Radio Communications Research Unit, CCLRC Chilbolton Observatory, Drove Road, Chilbolton, Hampshire, SO20 6BJ. (United Kingdom)

[3] Department of Meteorology, University of Reading, Reading, Berkshire, RG6 6BB. (United Kingdom)

[4] Met Office, FitzRoy Road, Exeter, Devon, EX1 3PB. (Formerly with the University of Reading) (United Kingdom)

## 1 Introduction

The Advanced Clear-air Radar for Observing the Boundary layer And Troposphere (ACROBAT), located at Chilbolton Observatory near Andover in southern England, is a fully-coherent, scanning, L-band, single-polarisation, pulse-compression Doppler radar. The radar was designed and constructed by members of the Radio Communications Research Unit, with assistance from the University of Reading and funding from UFAM, the Universities' Facility for Atmospheric Measurement.

At L-band wavelengths, radar backscatter from the clear atmosphere arises due to Bragg scattering from turbulent refractive index inhomogeneities. These Bragg returns make the 'clear-air' radar technique possible, whereby a sensitive radar can detect echoes from the air itself and thereby measure its motion. Since convection is associated with pronounced temperature and humidity gradients, ACROBAT has proved to be an excellent tool for studying convective structures in the boundary layer.

ACROBAT is a fully-coherent system, enabling it to accurately measure the phase of radar returns. By isolating the signals from stable ground-clutter targets, and by tracking their phase variation over time, changes in refractive index along the atmospheric paths to the targets can be monitored.

*Correspondence to:* Jon Eastment

J.D.Eastment@RL.AC.UK

This enables fields of refractivity variations to be derived. Since the radio refractive index of the atmosphere is highly dependent on humidity, refractivity measurements are extremely useful in tracking humidity anomalies associated with the onset of convection and precipitation.

In this paper, we present a block diagram-level description of the radar's engineering details, together with examples of data which illustrate typical measurement results. The system has recently been used to conduct an extensive series of observations to study atmospheric refractivity structure, boundary-layer evolution, convective development, and resulting storm morphology as part of the international collaborative 'Convective Storms Initiation Project', CSIP '05.

## 2 Radar overview and operating parameters

The ACROBAT radar system is based on a fully-steerable, 25 m-diameter, dish antenna; a travelling wave tube amplifier (TWTA) transmitter; a low-noise down-converter; and a flexible, programmable waveform generator and signal processor. The radar provides real-time measurement and display of the full Doppler spectrum, and of the spectral moments, reflectivity, Z; mean Doppler velocity, v; and spectral width, w. In addition to these processed parameters, raw time-series of in-phase and quadrature (I and Q) data may also be recorded for more detailed off-line analysis.

The radar operates at 1275 MHz, with a peak power of 1 kW at the feed and a system noise-figure of 3.5 dB. The 25m dish is illuminated with a horizontally-polarised dual-dipole / reflector feed, integrated with a Potter feed for the associated S-band 'CAMRa' radar (Goddard et al, 1994). Antenna gain

is 47.5 dBi, with a one-way –3 dB beamwidth of 0.7 degrees. The receiver is a single-conversion superhet, with a 60 MHz IF and 4 MHz IF bandwidth. Dual 12-bit ADCs, sampling at 2.5 MHz, are used to digitize I and Q video. Typically, data collection is conducted using a PRF of 2.5 kHz, with 8-bit BPSK complementary-coded transmit pulses of 6.4 microseconds total duration, corresponding to a maximum unambiguous range of 60 km and a range resolution of 120 m. Received signal processing comprises 8 coherent integrations, followed by a 256-point FFT, followed by 8 incoherent averages.

## 3 Detailed system description

### 3.1 Antenna and feed system

The antenna is a 25 m diameter fully-steerable parabolic dish with a dual-band, prime-focus feed system. The L-band feed consists of dual-dipoles with integral choke baluns. The choke-ring plate of the S-band scalar feed serves as a reflector at L-band. The dipoles are fed in-phase from a –3 dB Wilkinson power divider. A dual-slug tuner at the power divider input is used to achieve a very low input VSWR.

### 3.2 Transmit-receive duplexer unit

The TR-duplexer unit (Fig.1) is located in the dish's focus-cabin, adjacent to the feed. It employs a circulator to ensure high isolation between the radar's transmitter and receiver, whilst permitting both to share a common antenna. The unit provides transmitter harmonic filtering, power monitoring and damage protection in the event of an antenna fault. The receiver's low-noise amplifier (LNA) is protected from the high-power S-band radar pulses by a low-pass filter and Schottky-diode limiter. A PIN-diode transfer-switch is used to isolate and terminate the LNA input during the L-band transmit pulse. A preset attenuator sets overall front-end gain, while an isolator ensures that the LNA output is presented with a good impedance match.

**Fig. 1.** Block diagram of the TR-duplexer unit

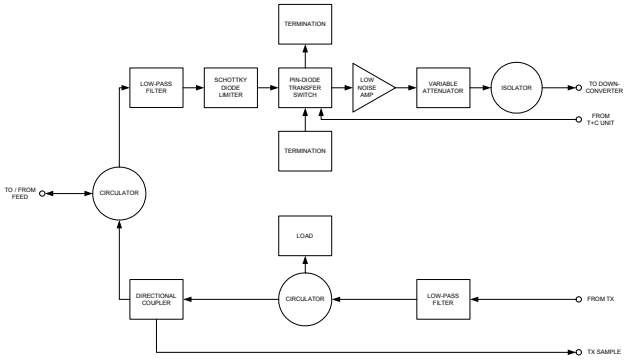


### 3.3 Receive down-converter

The down-converter (Fig. 2), located in the dish's radio-cabin, is a single-conversion superhet with a 60 MHz IF. The RF stage feeds a double-balanced diode-ring mixer via an isolator and image-rejecting inter-digital bandpass filter. A cascade of IF bandpass filters, IF amplifiers and a preset attenuator serve to define the IF bandwidth and conversion gain. The local oscillator (LO) is based on a programmable synthesizer. The synthesizer is phase-locked to a low phase-noise 10 MHz reference signal supplied from the control room. A 10 MHz bandpass filter removes wideband interference on the reference signal (due to the > 100 m cable-run from the control-room to radio-cabin), while a preset attenuator is used to set optimum reference signal level at the synthesizer's frequency reference input. A directional coupler permits LO signal monitoring, while a further preset attenuator enables drive level at the mixer's LO port to be optimized.

**Fig. 2.** Block diagram of the down-converter

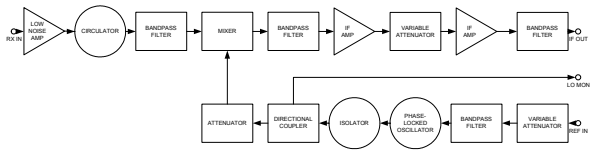


### 3.4 Receiver IF stages:

The receiver IF stages (Fig. 3) are located in the control-room. The IF signal from the down-converter is again bandpass filtered before entering a linear IF amplifier. The output from this amplifier is further filtered and attenuated to match the dynamic range of the following I/Q detector. The detector's I and Q outputs are separately low-pass filtered (to define the system video bandwidth), then level-shifted and amplified in a dual-channel video amplifier module. The outputs from the video amplifiers directly drive the ADC inputs of the data-acquisition (DAQ) system. The 60 MHz reference signal for the I/Q detector is derived from a phase-locked oscillator. This oscillator is locked to the radar's 10 MHz frequency standard. This standard is a high-stability, oven-controlled, SC-cut, quartz crystal oscillator. The signal from this oscillator is buffer-amplified, bandpass filtered, and distributed among various elements of the radar by a network of power dividers. Both the 10 MHz and 60 MHz signals may be monitored by means of directional couplers.

**Fig. 3.** Block diagram of the receiver IF stages

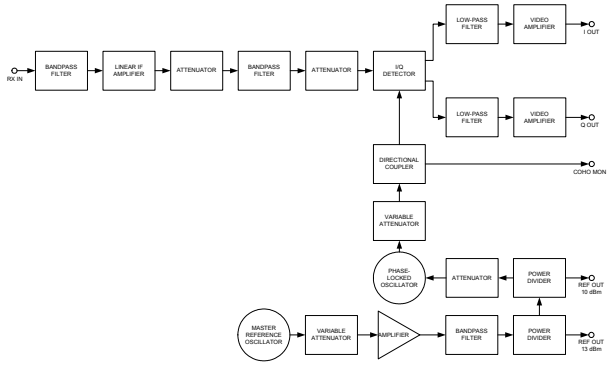


### 3.5 Exciter stages

The exciter stages (Fig. 4) are located in the control-room. They produce the low-level, pulse-compression coded, L-band drive signal for the following TWTA. They also provide clock and synchronization signals used by the radar's timing and control unit (TCU) and DAQ system. A network of power dividers distributes the 10 MHz reference frequency to a vector signal generator (VSG) and a pair of

function generators. One function generator is used to provide a TTL-level clock to the radar's timing and control unit. The other provides an ECL-level clock to an arbitrary waveform generator (AWG). The I and Q outputs from the AWG are used to modulate the VSG, so as to produce a coded L-band pulse. The VSG and AWG are programmed via a GPIB connection to the radar's control computer. The AWG's pulse-compression code is initiated by a trigger signal from the timing and control unit at the radar's pulse repetition frequency (PRF). The AWG also produces a synchronization pulse used by the DAQ system to determine the start of the pulse-compression code-cycle. An oscilloscope is used to verify the correct chip sequence within individual codes, and to monitor the progression of the code-cycle.

**Fig. 4.** Block diagram of the exciter stages

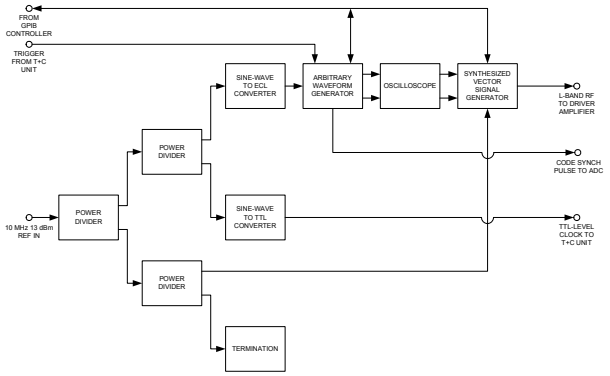


3.6 Transmit stages

The transmit stages (Fig. 5) are located in the dish's basement and radio-cabin. A low-power driver amplifier in the basement compensates for attenuation of the signal from the exciter in the ~100 m run of RG-214 cable from the control-room. A further RG-214 cable-run carries the signal from the output of the driver amplifier to the input of the TWTA, located in the radio-cabin. The TWTA produces amplified pulses of 2 kW peak-power at its output. It is connected via a high-power isolator (consisting of a circulator and high-power dummy-load) to the TR-duplexer unit in the focus-cabin via a Heliax cable-run of total attenuation ~3 dB. The cable-run comprises 2 fixed sections of LDF7-50A, together with a short, flexible section of FSJ4-50B around the dish's elevation axis. To facilitate transmitter performance monitoring, diagnostics and control, both the TWTA and a pulsed-power meter (connected via a directional coupler) are linked to the radar's control computer via the GPIB and a bus-extender module.

**Fig. 5.** Block diagram of the transmit stages

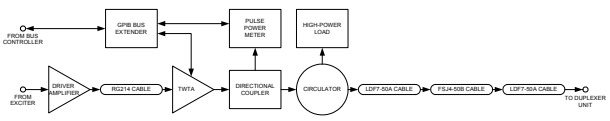


3.7 Timing, control and data acquisition system

Both the TCU and DAQ system are located in the control-room. The TCU is fed with a TTL-level 10 MHz reference signal from the exciter unit, and produces the radar's 'transmit fire' signal (at the PRF), the ADC sample clock, and several other system housekeeping signals (eg: the drive signal for the PIN-switch which protects the front-end LNA from damage during the transmit pulse). The DAQ system consists of 2 dual-channel, 12-bit ADC cards residing on the PCI-bus of the control PC. One pair of ADCs is used to digitize the I and Q signals from the receiver IF processor. Of the second pair of ADCs, one channel is used to detect the code synchronization pulse from the AWG, while the other channel is unused. A programmable ADC sample-timing card and a high-speed FIFO data-buffer / PCI-bus interface card complete the suite of cards comprising the DAQ hardware.

3.8 Pulse compression codes and signal processing

Whilst ACROBAT can use a wide variety of signal generation and processing schemes, the following pulse-compression code parameters (Spano and Ghebrebrhan, 1996) have been used for most of the work to date. The complementary code pair, A and B, have the following chip sequences: A = (-1, 1, 1, -1, -1, -1, -1, -1); B = (-1, -1, 1, 1, -1, 1, -1, 1). These codes are transmitted in the following sequence: ABBABAAB. Coherent integration over the 8-code sequence provides high levels of sidelobe cancellation for all Doppler velocities and spectral widths of interest for meteorological targets. Subsequent to pulse-compression processing and coherent integration, 256-point FFT processing is employed for Doppler analysis. Finally, for each FFT output bin, incoherent integration over 8 results is performed to reduce statistical noise in the final estimates.

3.9 Radar control and display system

The PC housing the DAQ cards (a 1.8 GHz Pentium 4, running under Linux) is also used for radar system configuration setup, data-collection operations and real-time display of results. Prior to the initial radar scan, the PC, via the GPIB, configures the VSG and AWG for the appropriate operating frequency and pulse-compression code parameters. PPI and RHI scans are then initiated from the operator's keyboard, and processed data are displayed in near real-time whilst the dish scans at a typical rate of 0.1° / second. Recorded data are written to a local server for archiving, while quick-look plots of Z, v and w are produced for off-line viewing via a web interface. ACROBAT is a flexible radar, exploiting largely software-defined signal generation and processing. Consequently, more specialized modes of radar operation, such as the collection of fixed-pointing spectral data, or the implementation of transmit sector-blanking (for interference mitigation), are readily catered for.

## 4 Examples of typical results

4.1 Observations of convection in the boundary-layer

ACROBAT receives returns due to both Rayleigh scatter from particulates and Bragg scatter. Bragg scatter returns arise from refractive index inhomogenities in the atmosphere primarily due to variations in water vapour content (Gossard and Strauch, 1983). This scattering mechanism is strongest at the edges of convective thermals where warm, moist air

within the thermal mixes with the cooler, dryer air surrounding the thermal as it rises. ACROBAT is therefore able to observe the top of the boundary layer and the development of convective elements. Fig. 6 shows Z, v and w for an RHI scan on 13th June 2005, where convective thermals were developing throughout the day due to solar heating of the surface. Since ACROBAT is mounted on the same dish as the S-band (10 cm wavelength) CAMRa radar, it is possible to determine if returns are due to Bragg or Rayleigh scatter. At S-band wavelengths, Bragg scatter echoes are approximately 14 dB weaker than at L-band wavelengths, while Rayleigh echoes are of the same intensity.

**Fig. 6.** Boundary layer convection observed by ACROBAT

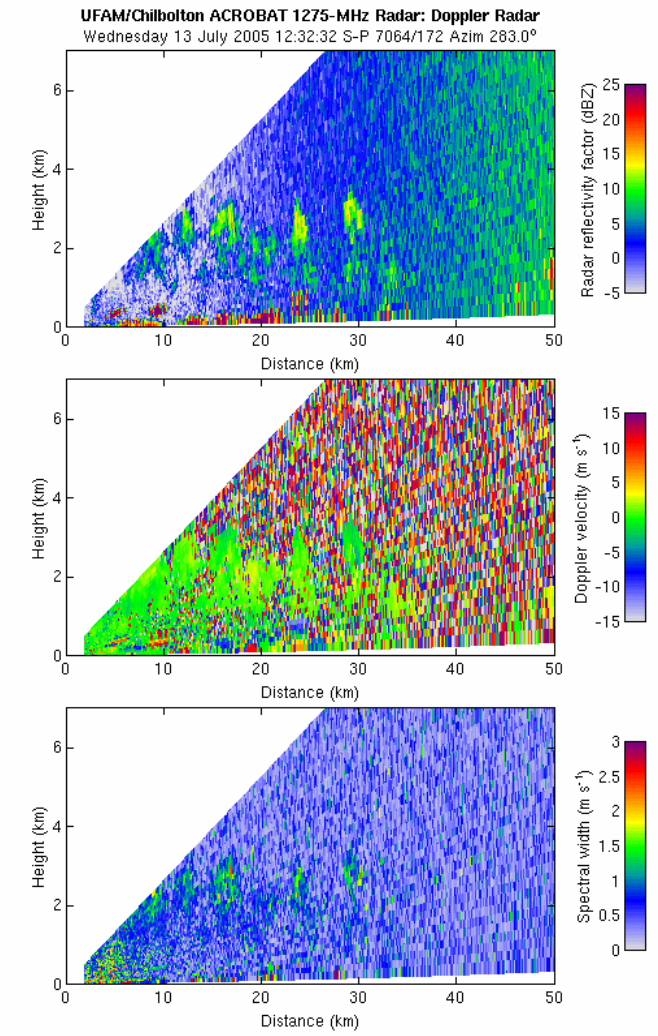


4.2 Temporal variation of atmospheric refractivity

ACROBAT has also been used to extract low-level refractivity fields. The technique (Fabry et al, 1997) uses changes in the absolute phase of returns from static ground targets to derive the refractivity field. Refractivity is strongly dependent on water vapour content (though also on temperature and pressure). As the refractivity measurements are representative of conditions just above the surface, these data may be used for studies of boundary-layer processes, frontal boundaries and storm outflows. Fig. 7 shows refractivity fields derived on 13th July 2005 separated by 40 minutes. Warm colours represent warm, dry air while cold colours represent cool, moist air. Here, one may observe the progress of a sea-breeze front as it propagates inland from the south coast of the UK.

**Fig. 7.** Time-evolution of refractivity observed by ACROBAT

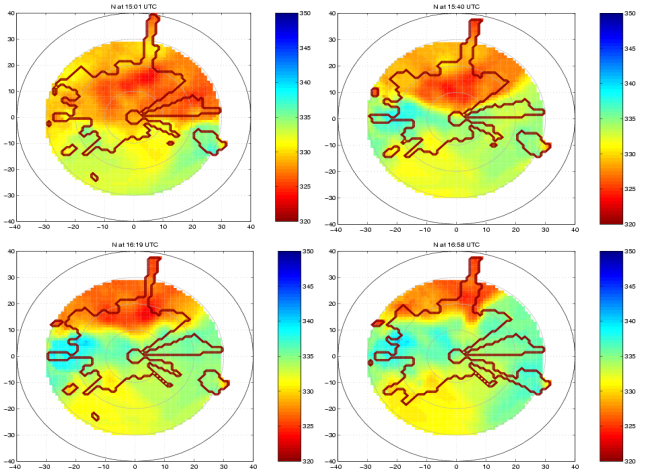

## 5 Conclusion

A block-diagram level description of the ACROBAT radar has been presented. The radar has proved to be a useful tool for investigating a variety of clear-air atmospheric phenomena.

*Acknowledgements:* The ACROBAT 1275 MHz radar is part of the UK Universities' Facility for Atmospheric Measurements (UFAM), funded by the NERC Joint Infrastructure Fund. The Chilbolton Facility for Atmospheric and Radio Research is a facility of the Council for the Central Laboratory of the Research Councils, CCLRC.

## References

Goddard, J. W. F., J. D. Eastment and M. Thurai, 1994: 'The Chilbolton Advanced Meteorological Radar: a tool for multidisciplinary atmospheric research'. *IEE Electronics and Communications Engineering Journal*, Vol. **6**, No. 2, 77-86.

Spano, E. and O. Ghebrebrhan, 1996: 'Complementary sequences with high sidelobe suppression factors for ST/MST radar applications'. *IEEE Trans. Geosci. Remote Sensing*, **34**, 317-329.

Gossard, E. E. and R. G Strauch, 1983: 'Radar observations of clear-air and clouds'. Elsevier Science Publications, Amsterdam.

Fabry, F., C. Frush, A. Kilambi and I. Zawadski, 1997: 'On the extraction of near-surface index of refraction using radar measurements of ground targets'. *J. Atmos. Oceanic Technol.*, **14**, 978-987.